SECONDARY TO PRIMARY RATIOS OF NUCLEI BELOW Z=30 IN A DYNAMIC SPIRAL-ARMED COSMIC RAY PROPAGATION MODEL

David Benyamin[1], Nir J. Shaviv[1], Tsvi Piran[1] & Ehud Nakar[2]
1. The Racah Institute of physics, The Hebrew University of Jerusalem, Jerusalem 91904, Israel
2. Raymond and Beverly Sackler School of Physics & Astronomy, Tel Aviv University, Tel Aviv 69978, Israel

Over the years, significant effort was devoted to understand cosmic ray propagation in the galaxy from the energy dependence of the secondary to primary ratios in galactic cosmic rays. We develop a fully three dimensional numerical code describing the diffusion of cosmic rays in the Milky Way. This code enables us to explore a model in which a large fraction of the cosmic ray acceleration takes place in the vicinity of galactic spiral arms and that these spiral arms are dynamic. Recently, the analysis of cosmic ray propagation from dynamic spiral arms was shown to have an important imprint on the Boron to Carbon ratio (Benyamin et al. 2014). We showed that the effect of having dynamic spiral arms is to limit the age of cosmic rays at low energies. This is because at low energies the time since the last spiral arm passage governs the Cosmic Ray (CR) age, and not diffusion. Using the model, the observed spectral dependence of the secondary to primary ratio is recovered without requiring any further assumptions such as a galactic wind, re-acceleration or various assumptions on the diffusivity. In particular, we obtain a secondary to primary ratio which increases with energy below about 1 GeV. We extended our previous model by upgrading the spallation network up to Silicon and including the Iron and sub-Iron elements (from Scandium to Nickel) necessary for simulating the sub-Iron to Iron ratio. We show that the latter ratio is consistently recovered with the same model parameters that explain the B/C ratio. We also empirically derive the energy dependent probability for K-capture isotopes by fitting the observed ^{49}Ti/^{49}V and ^{51}V/^{51}Cr ratios.

Particles Density Distribution

The CR density at the galactic plane for two energies. Clearly, the inhomogeneous source distribution gives rise to an inhomogeneous CR distribution in the galactic disk. Moreover, the effects of the different time scales is evident as well. At low energies, the spiral arm passage and escape time scales are comparable. This implies that the advection relative to the spiral arms becomes important, and one can see the ``smearing" associated with it. At high energies, the escape is much faster and one can consider the spiral arms to be effectively at rest.

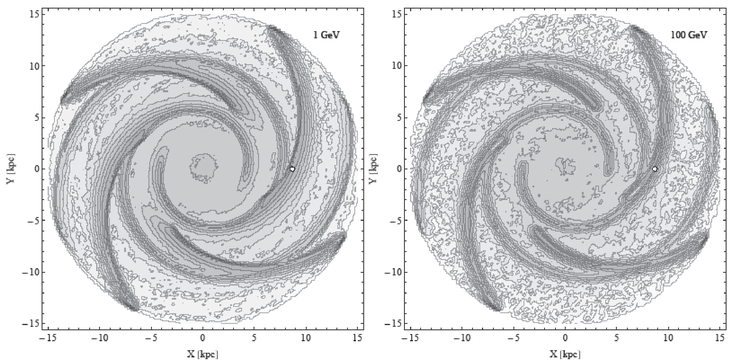

The relative CR density distribution in the Milky Way at two energies, normalized to the density at the location of the solar system. Left: At 1 GeV, Right: At 100 GeV. The contours are separated by 0.25 dex. The small circle denotes the location of the solar system. At low energies, the diffusion time scale and the time scale to escape the galaxy are comparable. As a consequence, it is possible to see the advection of the disk relative to the spiral arms. At higher energies, the escape is much faster and the advection cannot be seen.

An interesting result is the different spectral indices of CR inside and outside the spiral arms. A non-dynamic model can give no spectral difference. Here, however, the ratio between the density at different energies becomes location dependent, with the ratio becoming ``harder" in the spiral arms. For example, the ratio between 100 GeV CRs and 1 GeV CRs in the wake of the arms can be as large as $10^{0.5}$ lower. In other words, the spectral index can soften by about 0.25 when leaving the arms. This is consistent with observations of γ-ray emission, which show that the spectrum in the direction of the orion arm has a spectral index harder by 0.4 ±0.2 than in a high galactic latitude direction (rogers et al. 1999, Bloemen 1989).

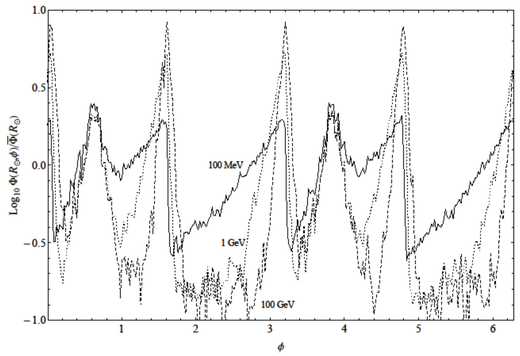

The flux $\Phi(R_\odot, \phi)$ at the galactic radius of the solar system as a function of the azimuthal angle, normalized to the average flux at this radius at the given energy. The solid line corresponds to the flux at 1 GeV, while the dashed to 100 GeV. Constraints based on Iron meteorites imply that the flux should vary by a factor of at least 2.5, between the spiral arms and the inter-arm region (Shaviv 2003).

Secondary to Primary particles Ratios

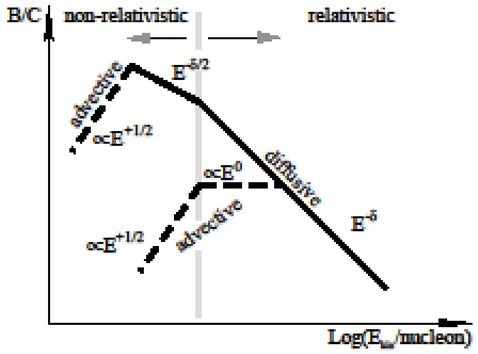

Heuristic description of the expected local interstellar secondary to primary ratio (Benyamin et al. 2014). The solid lines describe the limit in which CR diffusion dominates the age of the cosmic rays, while the dashed lines denote regions where advection from the spiral arm dominates the CR age. The two behaviors depend on whether the advection/diffusion change of behavior takes place for relativistic or non-relativistic particles. At low energies (below a few 100 Mev/n, this picture is modified due to Coulomb collisions in the ISM, and solar wind modulation).

Time scales

diffusion *advection*

$$\tau_s \approx \frac{s^2}{2D} \qquad \tau_{arm} \approx \frac{s/\sin i}{v_{arm}} \longrightarrow E_{break} \approx E_0 \left(\frac{s v_{arm} \sin i}{2D_0}\right)^{1/\delta}$$

Grammage correspond to the secondary to primary ratio

$$g \approx x\bar{\rho} \approx tv\bar{\rho}$$

diffusion *advection*

$$g_{\rm non-rel,diff} \propto \frac{\max(Z_h^2, sZ_h)}{E^{\delta/2}}\bar{\rho} \qquad g_{\rm non-rel,adv} \propto \frac{sv}{v_{arm}\sin i}\bar{\rho} \propto E^{1/2}$$

$$g_{\rm rel,diff} \propto \frac{\max(Z_h^2, s^2)}{E^{\delta}}\bar{\rho} \qquad g_{\rm rel,adv} \propto \frac{sc}{v_{arm}\sin i}\bar{\rho} \propto const.$$

Boron/Carbon

Comparison of our spiral-armed source distribution model to an azimuthally symmetric source distribution model. Shaded area correspond to the spectrum once solar wind modulation is added. The spiral-armed model agree with the observation in the high energy range and the low energy rangy. While the azimuthally symmetric agree with the observations only at the high energies. In the spiral-armed model the increasing ratio when the energy increase is due to the spiral arm effect and in the azimuthally symmetric model is due to Coulomb cooling. It can be seen that the Coulomb cooling cannot explain the low energies observations without additional effect.
(Our model parameters are not ideally and still need to do a full parameters study in order to get better results)

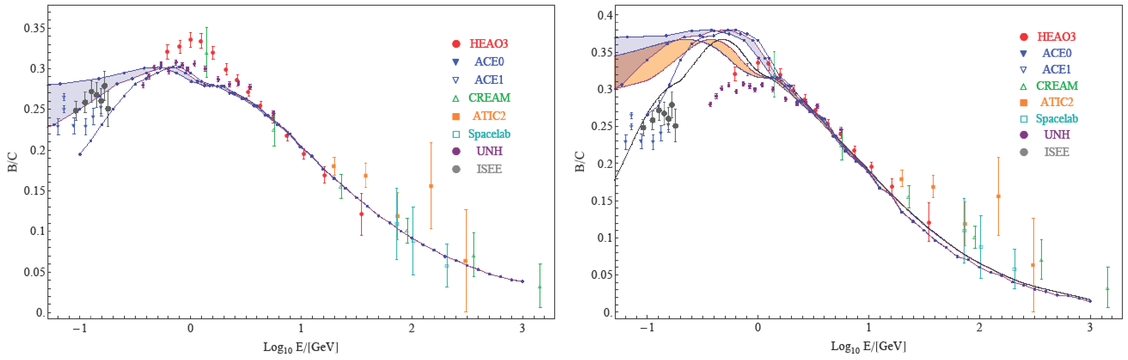

The Boron to Carbon ratio. Data obtained by HEAO-3 (Engelmann et al. 1990a), ACE (George et al. 2009), CREAM (Ahn et al. 2008), ATIC2 (Panov et al. 2008), spacelab (Swordy et al. 1990), UNH (Webber et al. 1985), ISEE (Krombel & Wiedenbeck 1988). Left: our nominal model results, right: an azimuthally symmetric source distribution model(dotted line and blue shading) having the same parameters as model GALPROP01000 of Strong & Moskalenko (1998) (smooth black line and orange shading). The shaded regions correspond to the spectrum once solar wind modulation is added, $(E/A)_{earth} = (E/A)_{ISM} - (Z/A)\cdot\Phi$. Typically, Φ ranges between 300 MV to 500 MV in the periods when the measurements are taken Usoskin et al. 2011, which is the range we take here.

Sub-Iron(Scandium+Titanium+Vanadium)/Iron(work in progress)

Here we compare the sub-Iron/Iron ratio between the two models which gave us the Boron/Carbon results(in this work, we still have problems with the cross-sections in the low energies, which gives a steep ratio decrease below few GeV). In the high energies , the spiral armed model can explain both the Boron/Carbon and the Sub-Iron/Iron ratio simultaneously with the same parameters. While in the azimuthally symmetric model, the results in the Sub-Iron/Iron are lower then the observations, which implies that the model needs more grammage to explain this ratio.

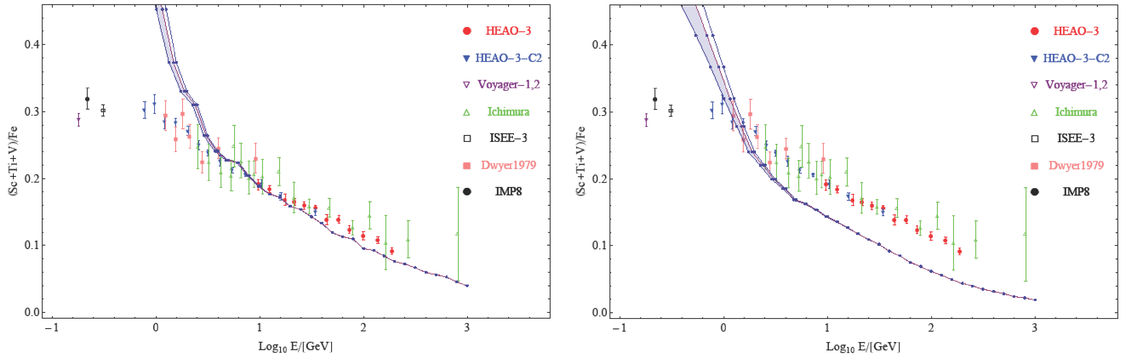

The sub-Iron(Scandium+Titanium+Vanadium)/Iron ratio . Data from references in Strong et al. (2007)). Left: our nominal model results, right: an azimuthally symmetric source distribution model with the parameters from mode number 01000 (Strong & Moskalenko 1998). It can be seen that the spiral-armed model agree with the observations and the azimuthally symmetric lower then the observations.

K-capture isotopes(work in progress)

At energies of few MeV the atoms starting to be ionized and at 1GeV they are almost completely strip of electrons. So the model should deal with a function that computes the chance the decay will occur. For the K-capture isotopes we calculate the chance the decay will occur by using the formula which we extrapolate :

$$P(E) = \begin{cases} 100\% & \text{if E} \le \text{a-b} \\ \frac{a}{b+E} & \text{if E} \ge \text{a-b} \end{cases}$$

P(E) is the chance that the EC decay will occur at a specific energy. a and b are parameters of this formula which we can change in order to fit the wanted ratios.
This formula means that below a certain energy(E = a-b) all the K-shell electrons are bound and the electron-capture will decay normally, and above this energy, the atoms starting to lose their K-shell electrons and have less chance to decay.
However we found this a=b=60MeV, are the best parameters for fitting the data of daughter EC isotopes to the EC isotopes ratios.

$$P = \frac{0.06GeV}{(0.06GeV + E)}$$

The logic behind this formula is that only when the energy is 0 the EC decay will happen at 100%, and the chance for the decay will occur decrease as the energy increase. But only at energies of few MeV the chance that the decay will occur start to decrease fast. Below few MeV, the atoms have all their K-shell electrons, so the chance of reactions is almost 100% of the reaction measured in the lab.

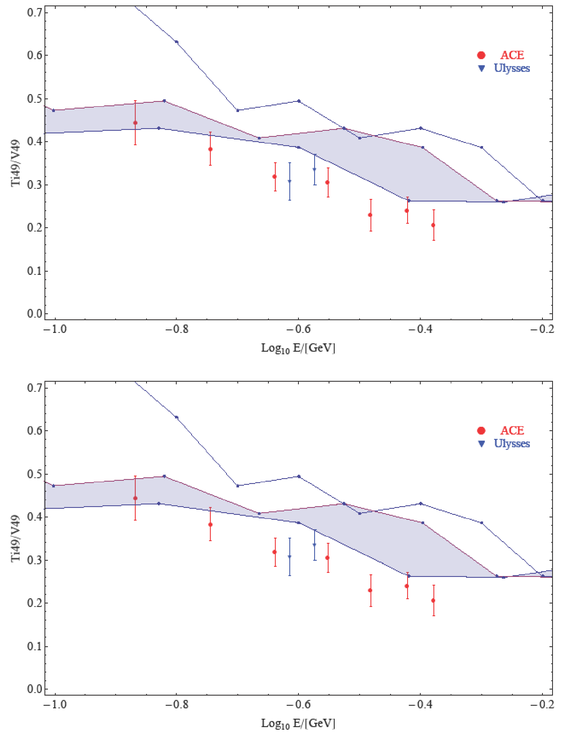

^{49}V and ^{51}Cr are isotopes that goes through EC reaction. Here we can see the ratios between their daughter isotope to them, ^{49}Ti/^{49}V and ^{51}V/^{51}Cr and the results we obtain in our nominal model. We used an empirical formula which calculates the chance of EC decay dependent on energy. There is not 100% agreement between the two ratios simultaneously and more careful analysis is needed to find a formula which might include a mass dependence. The shaded area is the correction to the simulation after solar modulation(in solar minima Φ=150MV and in solar maxima Φ=250MV). Data obtained by: see references in Jones et al. (2001)

David Benyamin
The Racah Institute of physics
The Hebrew University of Jerusalem
Jerusalem 91904, Israel

ACKNOWLEDGEMENTS
This work is supported by an Advanced ERC grant: GRB (DB and TP), by an ERC starting grant and ISF grant no. 174/08 (EN), and by the I-CORE Program of the Planning and Budgeting Committee and The Israel Science Foundation .(1829/12)